

Reaction $K^+p \rightarrow KN\pi\pi$ at 4.27 GeV/c incident momentum

N. M. Gelfand,* B. Lasinski,[†] P. Leary, F. Moser, A. Seidl,[‡] and J. Wolfson
*Enrico Fermi Institute and Department of Physics, The University of Chicago,
 Chicago, Illinois 60637*

J. Keren

Department of Physics, Northwestern University, Evanston, Illinois 60201
 (Received 23 February 1981; revised manuscript received 9 September 1982)

The cross sections for K^+p interactions at a center-of-mass energy of 3 GeV (4.3 GeV/c incident momentum) have been determined for the $K^+p\pi^+\pi^-$, $K^0p\pi^+\pi^0$, and $K^0\pi^+\pi^+n$ final states. The shape of the differential cross section $d\sigma/dt'$ for the quasi-two-body final state $K^{*0}(890)+\Delta^{++}(1236)$ is not a single exponential. Characteristics of the low-mass $K\pi\pi$ and $p\pi\pi$ enhancements are discussed.

I. INTRODUCTION

The interaction of K^+ mesons in a hydrogen bubble chamber has been extensively studied and many of the characteristics of the interaction have been reported.¹ The present experiment was designed to obtain knowledge of the details of the interaction. For this reason an experiment with high statistics at moderate energy was performed so that we could analyze a large number of events in the various reaction channels.

II. EXPERIMENTAL DETAILS

The 7° beam at the Argonne National Laboratory Zero Gradient Synchrotron was tuned to transport a 4.3-GeV/c K^+ beam to the Midwestern Universities Research Association—ANL 30-in. liquid-hydrogen bubble chamber. The μ and π contamination of the beam was monitored with a Cherenkov counter immediately before the chamber. The counting rate in the Cherenkov counter was consistent with the absence of any low-mass particles in the beam and we have therefore made no corrections for possible μ or π contamination in the beam. A total of 450×10^3 pictures were taken in two separate exposures.

The density of hydrogen was determined from the measured vapor pressure and temperature of the chamber. The density of the hydrogen was determined to be $\rho = 0.062 \pm 0.001$ g/cm³. The stated error in the density is an attempt to account both for the uncertainty in the operating conditions of the chamber and variation in the operating conditions during the run. The number of incident K^+ was

determined by counting beam tracks in every fiftieth frame. The total K^+ flux and density combine to give the sensitivity of the experiment as 7.37 ± 0.18 events/ μb .

Interactions of the K^+ mesons were located in a double scan of all the film. The scanning efficiency for all channels discussed here is $> 99\%$. The events were measured on manual digitizing projectors connected to an EMR-6050 computer. The measurements were analyzed by the computer at the time of measurement to ensure that the measurements were accurate. Tracks which failed the accuracy criteria were immediately remeasured. The geometric and kinematic reconstruction of events was performed off-line using standard programs.

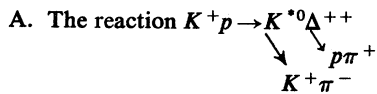
An event to be assigned to a given reaction hypothesis was required to have $\chi^2 < 20$ for four-constraint (4C) fits. In addition the ionization density calculated from the mass, momentum, and dip angle for all tracks had to agree with the ionization estimates made by the measurer for a hypothesis to be accepted. As a result of the kinematic fits, events were assigned to particular reaction channels.

III. THE REACTION $K^+p \rightarrow KN\pi\pi$

The four-body final states have been studied extensively in K^+p interactions.² The principal features of the final states are well known: large cross sections for production of the $K^*(890)$ and the $\Delta(1236)$, and low-mass enhancements in the $(K\pi\pi)^+$ and $(N\pi\pi)^+$ mass spectra. Cross sections for the various reaction channels observed in four-body final states are found in Table I.

TABLE I. Cross sections for $K^+p \rightarrow KN\pi\pi$.

Reaction	Observed events	Cross section (mb)
$K^+p \rightarrow K^+p\pi^+\pi^-$	14 648	1.988 ± 0.051
$K^+p \rightarrow K^*(890)\pi^+p$ $\quad \quad \quad \searrow K^+\pi^-$	8053	1.09 ± 0.03
$K^+p \rightarrow K^*(1420)\pi^+p$ $\quad \quad \quad \searrow K^+\pi^-$	1015	0.138 ± 0.010
$K^+p \rightarrow K^*(890) + \Delta^{++}(1236)$ $\quad \quad \quad \searrow K^+\pi^- \quad \quad \searrow p\pi^+$	4883	0.663 ± 0.044
$K^+p \rightarrow K^*(1420) + \Delta^{++}(1236)$ $\quad \quad \quad \searrow K^+\pi^- \quad \quad \searrow p\pi^+$	915	0.124 ± 0.006
$K^+p \rightarrow \Delta^{++}(1236)K^+\pi^-$ $\quad \quad \quad \searrow p\pi^+$	8430	1.14 ± 0.05
$K^+p \rightarrow K^0p\pi^+\pi^0$	3506	1.456 ± 0.085
$K^+p \rightarrow K^*(890)\pi^+p$ $\quad \quad \quad \searrow K^0\pi^0$	1023	0.425 ± 0.041
$K^+p \rightarrow K^*(890)\pi^0p$ $\quad \quad \quad \searrow K^0\pi^+$	922	0.383 ± 0.039
$K^+p \rightarrow \Delta^{++}(1236)K^0\pi^0$ $\quad \quad \quad \searrow p\pi^+$	1235	0.513 ± 0.044
$K^+p \rightarrow \Delta^+(1236)K^0\pi^+$ $\quad \quad \quad \searrow p\pi^0$	354	0.147 ± 0.022
$K^+p \rightarrow \rho^+K^0p$ $\quad \quad \quad \searrow \pi^+\pi^0$	441	0.183 ± 0.023
$K^+p \rightarrow K^0n\pi^+\pi^+$	1189	0.483 ± 0.036
$K^+p \rightarrow K^*(890)\pi^+n$ $\quad \quad \quad \searrow K^0\pi^+$	544	0.221 ± 0.023
$K^+p \rightarrow \Delta^+(1236)K^0\pi^+$ $\quad \quad \quad \searrow n\pi^+$	205	0.083 ± 0.017



The differential cross section $d\sigma/dt'$ for the $K^*\Delta^{++}$ channel in the $K^+\pi^-\pi^+p$ final state is plotted in Fig. 1. The data cannot be fit with a single exponential, i.e., $d\sigma/dt' \neq Ae^{-bt'}$, because of the very sharp forward peak and the more gradual fall-off at larger t' .³ Many functional forms can be used to fit the distribution. We have used the form

$$d\sigma/dt' = A_1 e^{b_1 t'} + t' A_2 e^{b_2 t'}$$

The results of the fit are shown in Table II. The slope associated with the forward peak $b_1 = 14.5 \pm 3 \text{ GeV}^{-2}$ is much steeper than is usually encountered in either elastic scattering or quasi-two-body production experiments.⁴ We believe that the shape of the differential cross section suggests that the production mechanism at small t' is different from that

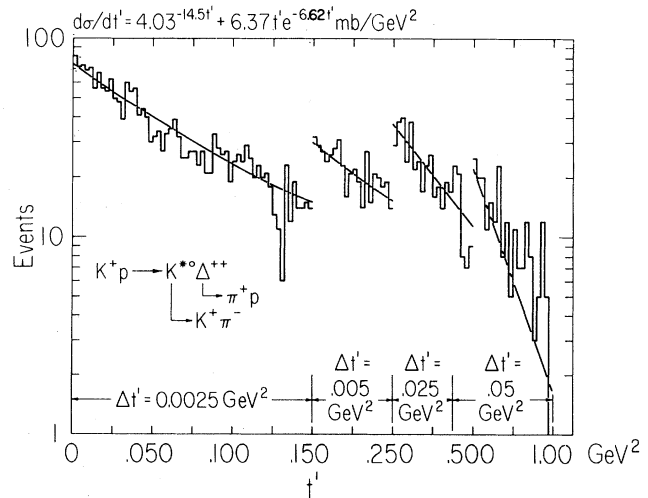


FIG. 1. $d\sigma/dt'$ for $K^{*0}\Delta^{++}$ ($K^* \rightarrow K^+\pi$, $\Delta^{++} \rightarrow p\pi^+$) events.

TABLE II. Values for the parameters in a fit to $d\sigma/dt'$ of the form $A_1 e^{-b_1 t'} + t' A_2 e^{-b_2 t'}$ for the reaction $K^+p \rightarrow \Delta^{++}(1236) + K^*(890)$, $\Delta^{++} \rightarrow p\pi^+$, $K^* \rightarrow K + \pi^-$.

$A_1 = 4.03 \pm 0.14$ mb/GeV ²	$b_1 = 14.46 \pm 0.035$ GeV ⁻²
$A_2 = 6.37 \pm 0.18$ mb/GeV ⁴	$b_2 = 6.62 \pm 0.04$ GeV ⁻²

at large t' .

Information about possible production mechanisms of a resonance is obtained from the decay of the resonance. To study the decay of a resonance we compute the moments of the real part of the spherical harmonics $\text{Re}(Y_l^m)$ about the axes suggested by Gottfried and Jackson.⁵ For values of $l > 2$ the moments for the decay of both the K^* and the Δ are consistent with being zero.

In Fig. 2 we plot the decay moments for $l \leq 2$ of the K^* and the Δ^{++} as a function of t' . All moments with $m \neq 0$ are consistent with zero for $t' < 0.024$ GeV². For $t' > 0.024$ GeV² the $l=1, m=1$ moment for K^* (890) decay is different from zero.

The one-pion-exchange model has long been invoked as the mechanism for the reaction $K^+p \rightarrow K^*\Delta$ at small t (and therefore at small t'). This model requires that the moments with $m \neq 0$ be zero and our data are consistent only at very small t' , $t' < 0.024$ GeV², with this prediction of the one-pion exchange hypothesis.

B. The Q and $N(1570)$

We observe low-mass enhancements in the $K^+\pi^+\pi^-$, $K^0\pi^0\pi^+$, and $p\pi^+\pi^-$ mass distributions (Fig. 3). These are due to the well established Q and $N(1570)$ resonances. The Q region does not show the narrow peaks reported in experiments at other energies (Ref. 6).

The Q region has been subjected to an elaborate partial wave analysis (Ref. 7) which our data do not justify repeating. We have however fit the distribution of events on the $K\pi\pi$ Dalitz plot in an attempt to measure the relative decay rates into $K^*\pi$ and $K\rho$. We have found that the relative rates are very sensitive to the way that ambiguous events are handled. The 4C fits to the reaction $K^+p \rightarrow K^+p\pi^+\pi^-$ are sometimes (approximately 7% of the events) ambiguous in the identification of the π^+ and the K^+ .⁸ These ambiguous events are not distributed uniformly in the $K\pi\pi$ mass distribution, but are concentrated in the Q region. We believe that proper analysis of the Q region requires a correct handling of ambiguous events. Our procedure is described in Ref. 8.⁹ Using that method

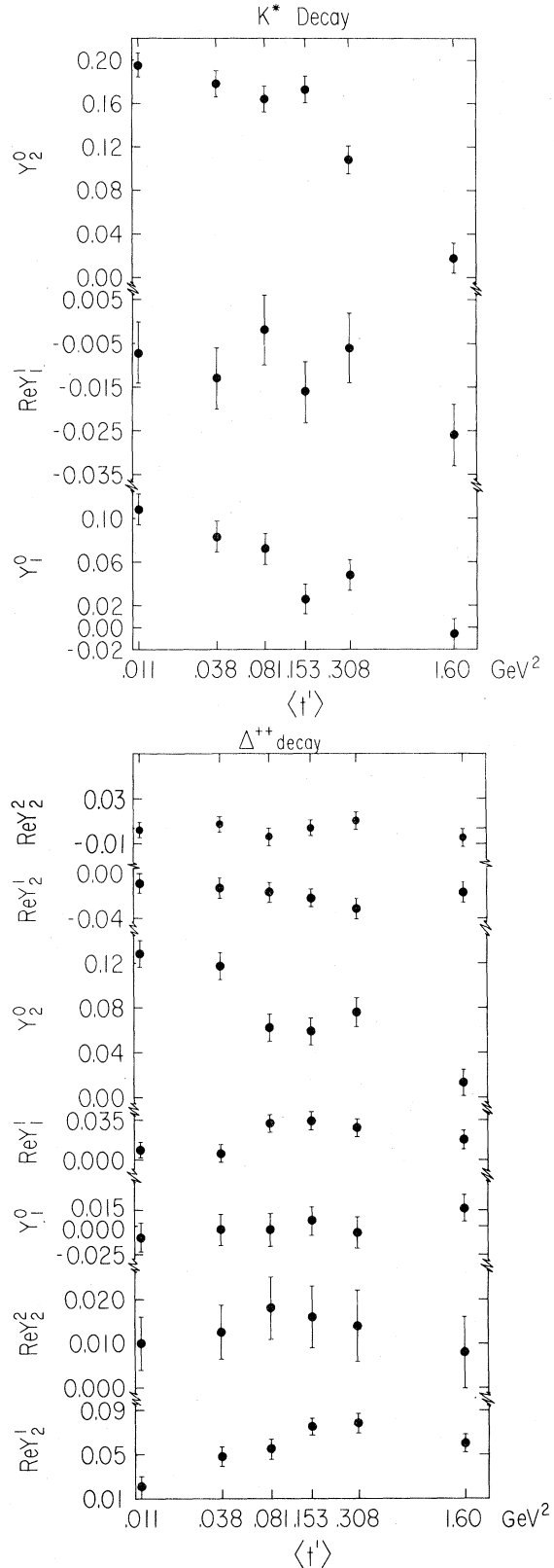


FIG. 2. Decay moments of the $K^{*0} (\rightarrow K^+\pi^-)$ and $\Delta^{++} (\rightarrow p\pi^+)$.

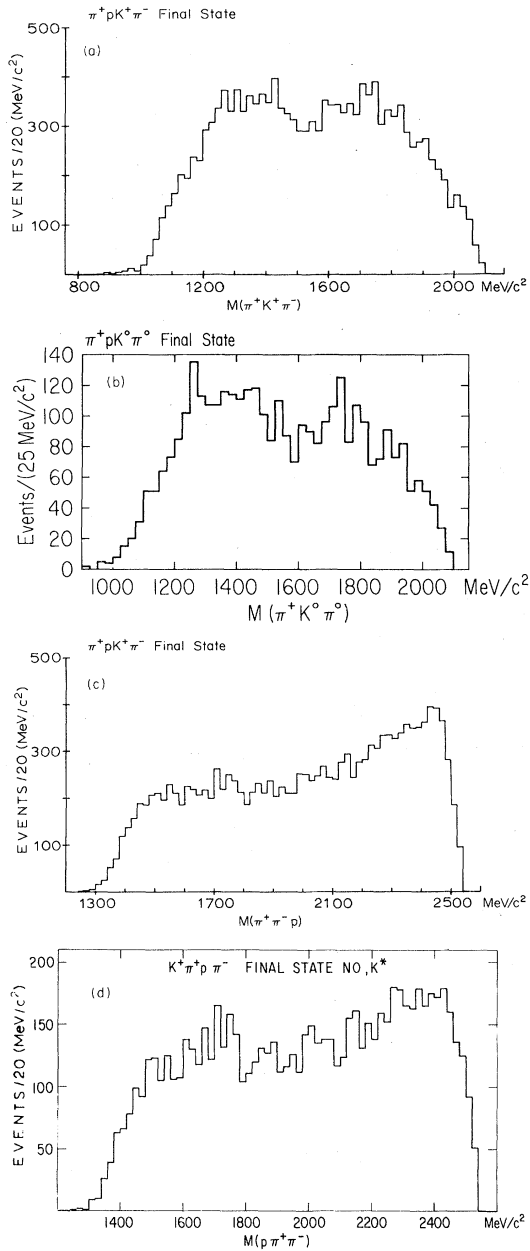


FIG. 3. (a) The $K^+ \pi^+ \pi^-$ mass spectrum from the reaction $K^+ p \rightarrow K^+ p \pi^+ \pi^-$. (b) The $K^0 \pi^0 \pi^+$ mass spectrum from the reaction $K^+ p \rightarrow K^0 p \pi^+ \pi^0$. (c) The $\pi^+ \pi^-$ mass spectrum from the reaction $K^+ p \rightarrow K^+ p \pi^+ \pi^-$. (d) The $p \pi^+ \pi^-$ mass spectrum after removing the $K^*(890)$.

for resolving ambiguities we have fit the distribution of events on the Dalitz plot for different intervals of $K^+ \pi^+ \pi^-$ mass. No significant variation in the branching ratios, which could be indicative of

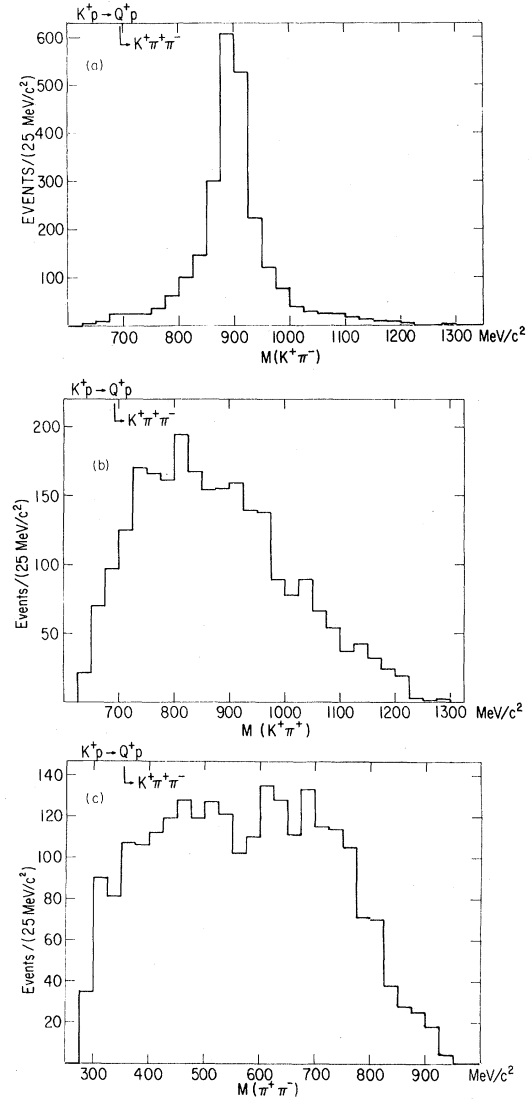


FIG. 4. The $Q^+ \rightarrow K^+ \pi^+ \pi^-$. $M(K^+ \pi^+ \pi^-) < 1470 \text{ MeV}/c^2$, $t_p' < 0.45 \text{ GeV}/c^2$, no Δ^{++} events. (a) $K^+ \pi^-$ mass spectrum. (b) $K^+ \pi^+$ mass spectrum. (c) $\pi^+ \pi^-$ mass spectrum.

structure in the $K^+ \pi^+ \pi^-$ mass distribution, was found. The results of a fit to the projections of (Figs. 4 and 5) the $K^+ \pi^+ \pi^-$ and $K^0 \pi^0 \pi^+$ Dalitz plots to an incoherent sum of $K^* \pi$, $K \rho$, and flat background are given in Table III. The much larger background observed in the $K^0 \pi^0 \pi^+$ decay mode of the Q^+ makes a direct comparison of the ratio $K^* \pi / K \rho$ for the different decay modes of the Q^+ difficult. It is clear, however, that the $K \rho$ decay is far more prominent in the $K^0 \pi^0 \pi^+$ final state.

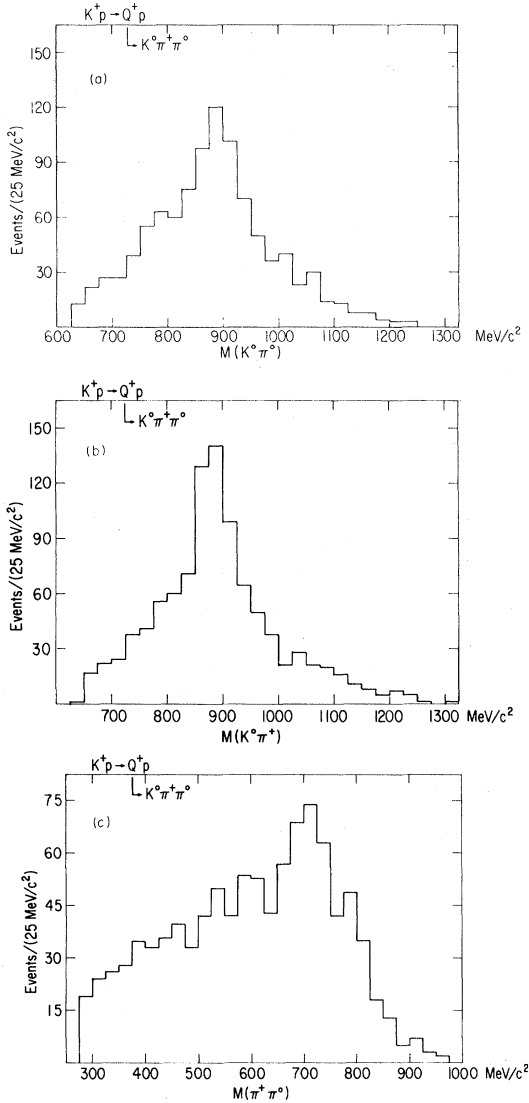


FIG. 5. $Q^+ \rightarrow K^0\pi^0\pi^+$. $M(K^+\pi^+\pi^-) < 1470$ MeV/c², $t'_p < 0.45$ GeV/c², no Δ^{++} events. (a) $K^0\pi^0$ mass spectrum. (b) $K^0\pi^+$ mass spectrum. (c) $\pi^+\pi^0$ mass spectrum.

A similar fit has been done for a sample of $N(1570)$ events. We have selected events with $M(p\pi^+\pi^-) < 1870$ MeV/c² with no $K^*(890)$ and $t_{KK'} < 0.45$ GeV² and $t'_{p\Delta} < 0.6$ GeV² to enhance the $N(1570)$ signal relative to the background. The pro-

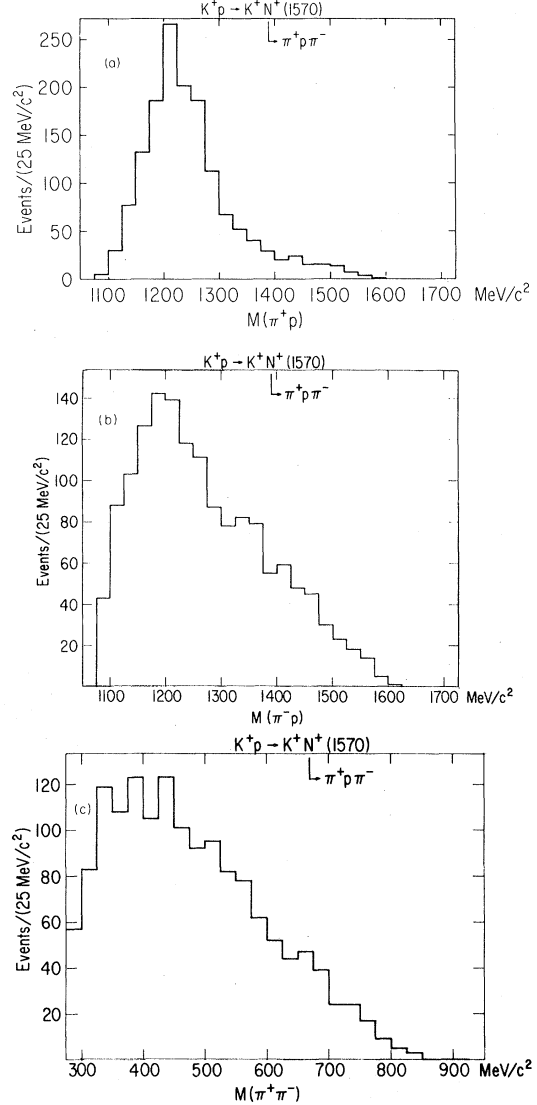


FIG. 6. The decay $N(1570) \rightarrow p\pi^+\pi^-$. $M(p\pi^+\pi^-) < 1870$ MeV/c², $t'(KK) < 0.45$ GeV², $t'(p,\Delta^{++}) < 0.6$ GeV², no K^* events. (a) π^+p mass spectrum. (b) π^-p mass spectrum. (c) $\pi^+\pi^-$ mass spectrum.

jections of the $N(1570)$ decay are shown in Fig. 6. A fit of the distribution on the Dalitz plot gives a ratio of $\Delta^{++}\pi:\Delta^+\pi^+ = (3.5 \pm 1.3):1$ which is in agreement with the usual $T = \frac{1}{2}$ assignment for the $N(1570)$.

TABLE III. Fractional decay modes for the Q^+ .

	$K^*\pi$	$K\rho$	Background
$Q^+ \rightarrow K^+\pi^+\pi^-$	0.841 ± 0.02	0.091 ± 0.05	0.061 ± 0.02
$Q^+ \rightarrow K^0\pi^0\pi^+$	0.521 ± 0.05	0.351 ± 0.09	0.131 ± 0.05

IV. CONCLUSIONS

The reaction $K^+p \rightarrow KN\pi\pi$ is dominated by copious production of two- and three-body resonances. The differential cross section $d\sigma/dt'$ for the quasi-two-body reaction $K^+p \rightarrow K^*\Delta^{++}$ cannot be fit

with a single exponential because of a very steep falloff at small t' . The broad enhancements in the $K\pi\pi$ and $N\pi\pi$ final states have $T = \frac{1}{2}$ and no obvious structure. The decay of these resonances is predominantly into quasi-two-body systems.

ACKNOWLEDGMENT

This work was supported in part by the National Science Foundation.

*Present address: Fermi National Accelerator Laboratory, Batavia, IL 60510.

†Present address: Lawrence Livermore Laboratory, Livermore, CA 94550.

‡Present address: University of Michigan, Ann Arbor, MI 48109.

¹A list of references to experiments involving K^+p interaction is contained in Particle Data Group, Report No. LBL-90, 1978 (unpublished).

²Here too Ref. 1 contains a list of references. Among these the following contain material related to the topics discussed in this paper. (a) G. Goldhaber *et al.*, Phys. Lett. **6**, 62 (1963); (b) G. Abrams *et al.*, Phys. Rev. D **1**, 2433 (1970); (c) B. Forman *et al.*, *ibid.* **3**, 2610 (1971); (d) D. Colley *et al.*, Nucl. Phys. **B55**, 1 (1973); (e) K. Barnham *et al.*, *ibid.* **B25**, 49 (1979); (f) J. Berlinghieri *et al.*, *ibid.* **B8**, 333 (1968); (g) C. Chien *et al.*, Phys. Lett. **28B**, 143 (1968); (h) M. Matison

et al., Phys. Rev. D **19**, 1872 (1974); (i) R. K. Carnegie *et al.*, Nucl. Phys. **B127**, 509 (1977); (j) P. Estabrooks, *et al.*, *ibid.* **B133**, 490 (1978).

³A similar effect was seen in the reaction $\pi^+p \rightarrow \rho^0\Delta^{++}$ which is also regarded as dominated by one-pion exchange [J. Prentice *et al.*, Nucl. Phys. **B35**, 79 (1971)].

⁴A. Seidl, Phys. Rev. D **7**, 621 (1973).

⁵K. Gottfried and J. D. Jackson, Nuovo Cimento **33**, 309 (1964).

⁶Reference 2(e); G. Alexander *et al.*, Nucl. Phys. **B13**, 503 (1969).

⁷For a different method of analysis, see G. W. Brandenburg *et al.*, Phys. Rev. Lett. **36**, 703 (1976); **36**, 706 (1976).

⁸B. Forman *et al.*, Phys. Rev. D **3**, 2610 (1971).

⁹We do not find any discussion of how any ambiguous events were handled in Ref. 7.